Dynamics of Solar and Stellar Convection Zones and Atmospheres
Proceedings IAU Symposium No. 365, 2024
A. V. Getling & L. L. Kitchatinov, eds.
doi:10.1017/S1743921324000097

Nonlinear and stochastic mechanisms of the solar cycle and their implications for the cycle prediction

Jie Jiang

School of Space and Environment, Beihang University, Beijing, People's Republic of China, email: jiejiang@buaa.edu.cn
Key Laboratory of Space Environment Monitoring and Information Processing, Ministry of Industry and Information Technology, Beijing, China

Abstract. Solar activity shows an 11-year (quasi)periodicity with a pronounced, but limited variability of the cycle amplitudes. The properties of active region (AR) emergence play an important role in the modulation of solar cycles and are our central concern in building a model for predicting future cycle(s) in the framework of the Babcock–Leighton (BL)-type dynamo. The emergence of ARs has the property that strong cycles tend to have higher mean latitudes and lower tilt angle coefficients. Their non-linear feedbacks on the solar cycle are referred to as latitudinal quenching and tilt quenching, respectively. Meanwhile, the stochastic properties of AR emergence, e.g., rogue ARs, limit the scope of the solar cycle prediction. For physics-based prediction models of the solar cycle, we suggest that uncertainties in both the observed magnetograms assimilated as the initial field and the properties of the AR emergence should be taken into account.

Keywords. Solar cycle, Solar dynamo, Cycle prediction, Stochastic noise

1. Introduction

Predicting the solar cycle is crucial in our technological society. Many attempts were made to predict cycle 25, including empirical and physical methods to determine its amplitude and cycle profile. There are also several comprehensive reviews about the solar cycle prediction including predictions of cycle 25, e.g., Petrovay (2020); Nandy (2021); Jiang et al. (2023); Bhowmik et al. (2023); Penza et al. (2023). Here no additional cycle 25 predictions or reviews are required. Figure 1 displays the time evolution of the polar field (upper panels) and longitudinally averaged surface field (lower panels) from Wilcox Solar Observatory (WSO, left panels) and SDO/HMI (right panels) data. Both datasets indicate that the polar field reversal began in mid-2023. As of the end of 2023, both the northern and southern polar regions have the magnetic field polarity of cycle 25. The polar reversal indicates that cycle 25 has reached its maximum phase since mid-2023. The maximum phase usually persists about two years. The amplitude of the ongoing cycle 25 is about 125. The result is in agreement with what we once suggested when we investigated the predictability of the solar cycle (Jiang et al. 2018).

Physics-based predictions of the solar cycle provide an effective means of verifying our understanding of it. Numerical weather forecasting provides a good model for physics-based solar cycle predictions. In the 1960s, Lorenz demonstrated the significance of nonlinear dynamics in the context of convecting systems, opening the door to physics-based weather forecasting. (Lorenz 1963, 1965, 1969). Lorenz's discovery regarding the predictability of weather showed that chaotic dynamics result from nonlinearity. It is

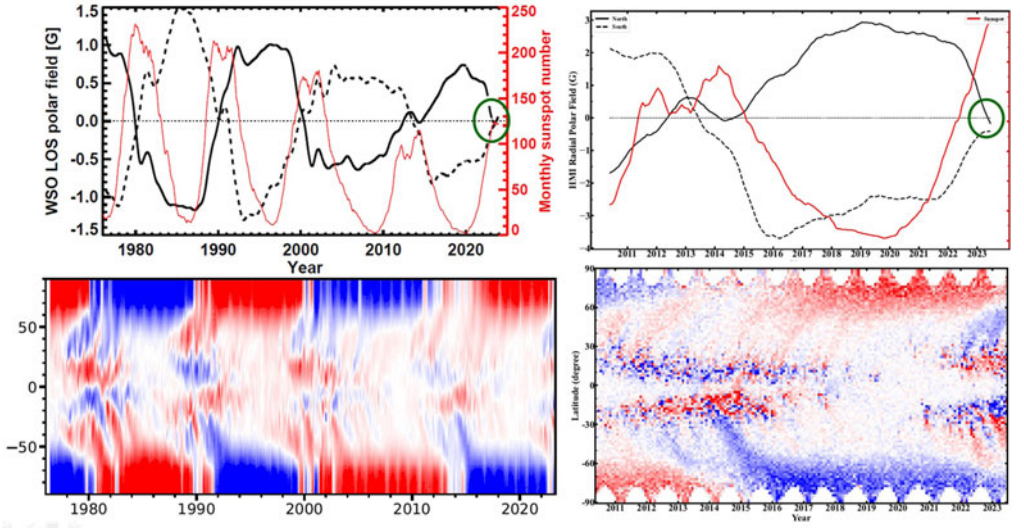

Figure 1. Illustration of the recent polar field reversals with data from WSO (left panels) and from HMI/SDO (right panels). The red curves shown in the top panels are the 13-months smoothed sunspot numbers (version 2.0). Black solid and dashed curves are the northern and southern polar fields, respectively. WSO (left) and HMI (right) polar field is defined as the average of the line-of-sight field between about 55° latitude and the poles and the average of the radial field between 60° and 70° latitudes,respectively. The lower panels show the longitudinal averaged solar surface field during 1976-2023 (left panel) and during 2010-2023 (right panel). Courtesy of the datasets from WSO, HMI/SDO, and SIDC sunspot number.

now known that the atmosphere's chaotic nature limits weather forecasts to about two weeks, even with ideal models and perfect observations.

The sunspot number time series shows the variability of solar cycles, including the odd-even effect, also known as the Gnevyshev–Ohl (G-O) rule (Gnevyshev and Ohl 1948). This pattern is characterized by alternating higher and lower than average solar cycle amplitudes observed in the sunspot number record. However, some cycles do not follow this rule. The variability of the solar cycle indicates that there are nonlinear or stochastic mechanisms that modulate solar cycle amplitudes. However, it is unclear which mechanism is dominant. The investigation of the G-O rule could provide insights into the nature of solar cycle variability. Understanding the nature of solar cycle variability is essential for predicting solar cycles accurately.

2. Understanding the nature of solar cycle variability

There is increasing evidence to support the idea that the solar dynamo is of the Babcock–Leighton (BL) type, as proposed by (Babcock 1961; Leighton 1969). According to the BL-type models, sunspot-generating surface eruptions of the toroidal magnetic field are the source of the poloidal field. The dynamo loop corresponds to the regeneration of the poloidal and toroidal fields. The toroidal field is generated from the poloidal field due to differential rotation. The observed torsional oscillation is approximately 0.5% of the average rotation rate (Howe 2009). Therefore, the process of the toroidal field generation can be regarded as a linear one, which is also supported by the correlation between the polar field at cycle minimum and the subsequent cycle strength (Jiang et al. 2007; Wang and Sheeley 2009). The generation of the poloidal field from the toroidal field by the BL processes is expected to include nonlinear and stochastic mechanisms. The emergence and evolution of ARs can be observed. Given that the generation of the

https://doi.org/10.1017/S1743921324000097 Published online by Cambridge University Press

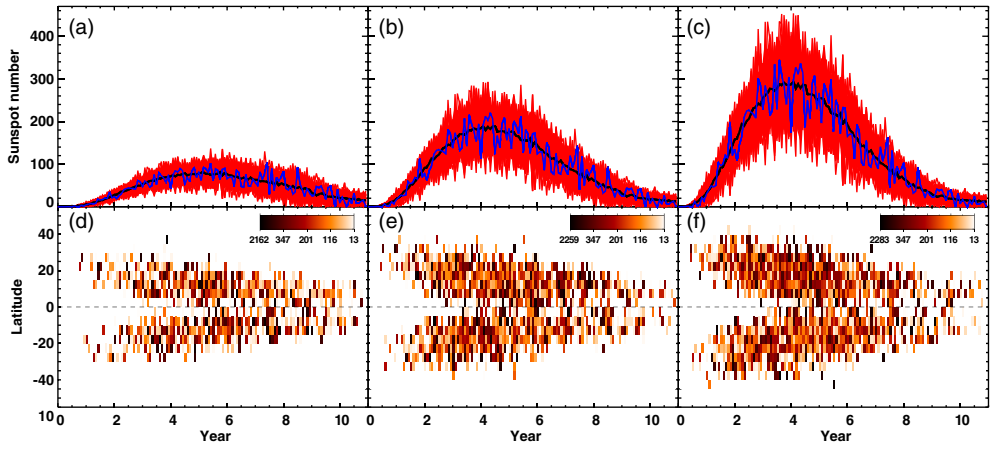

Figure 2. Examples of synthetic solar cycles of different amplitudes S_n. Top: Time evolution of the synthetic sunspot number. Red curves show the 100 simulated random realizations. Black indicates the expected sunspot number value at each time. The blue curve marks one of the random realizations. Bottom: Time evolution of the sunspot emergence latitude for the cases shown using blue curves. The color displays the average area in unit of MSH in bins of one month by 5 degrees in latitude. From left to right S_n=70, S_n=180, and S_n=280, respectively. Image reproduced with permission from Jiang (2020), copyright by the American Astronomical Society.

toroidal field is a linear process, understanding solar variability may only require processes over the solar surface with well-measured empirical relations for AR emergence and evolution. An interior dynamo model is not particularly useful in understanding the nature of solar cycle variability at present since the process of flux emergence remains an outstanding question.

ARs are characterized by the tilt of the line connecting their two polarities, which typically deviates from the east-west direction. This tilt angle introduces the poloidal component. The poloidal field contribution, usually measured by the quality axial dipole moment, is roughly proportional to the flux and tilt of the sunspot upon emergence (Wang and Sheeley 1991). However, it is important to note that surface flux transport processes that occur after the emergence of sunspot groups have the potential to significantly alter the dipole moment (Jiang et al. 2014; Petrovay et al. 2020; Wang et al. 2021). These processes can be simulated using surface flux transport models (Jiang et al. 2014; Yeates et al. 2023). This raises the question of whether observable properties of sunspot emergence are subject to nonlinear and stochastic mechanisms that modulate solar cycles.

Now let's first see the systematic property of the sunspot emergence. Past studies shows a good correlation between the mean latitude of sunspot emergence during a cycle and the cycle strength (Li et al. 2003; Solanki et al. 2008; Jiang et al. 2011). Strong cycles tend to have higher latitude emergence. Now let's see the effect of the systematic property on the solar cycle. For each sunspot group, net flux transported across the equator determines the final contribution to the dipole field. Lower latitude emergence tends to finally contribute more to the axial dipole field. Together with the statistical relation that stronger cycles tend to higher mean latitudes of ARs, the systematic properties of AR emergence in latitude work as a nonlinearity to modulate the dipole field generation. We refer to it as latitudinal quenching (Jiang 2020; Petrovay 2020; Karak 2020).

Besides the latitude, the tilt angle is another key parameter of an active region. The anti-correlation between the tilt angle and the cycle strength found by Dasi–Espuig et al.

https://doi.org/10.1017/S1743921324000097 Published online by Cambridge University Press

(2010) initiated the revival of the Babcock–Leighton type dynamo during the past decade. However, the standard errors of the averaged tilt angle for each cycle are significant, and the anti-correlation is mainly due to cycle 19. Recently, Jiao et al. (2021) discovered a strong anti-correlation between the tilt coefficient and the cycle strength by improving the method of dealing with historical data. This anti-correlation can modulate the generation of the dipole field, as the dipole field is proportional to the tilt angle. The phenomenon is referred to as tilt quenching.

Apart from the systematic property of the tilt angle, there is a large scatter in tilts resulting from randomness due to convective flows (Weber et al. 2011). The dependence of the tilt scatter on the umbra area can be measured using historical datasets. Any variation in the properties of the spots, such as emergence latitude or tilt angle, introduces a corresponding variation in the resulting poloidal field and, consequently, in the amplitude of the subsequent cycle.

In summary, both stochastic and systematic properties are involved in sunspot emergence in their tilt angle, latitude, area, and number. Jiang et al. (2011, 2018) gave empirical formula describing relations between sunspot emergence and cycle strength. Hence, with a given cycle strength, we may synthesize the sunspot emergence.

Figure 2 adapted from Jiang (2020) displays three examples of synthetic solar cycles with weak, medium, and strong amplitudes, respectively. For each cycle amplitude, we generate 100 random realizations including the number, latitude, longitude, tilt, and area of each AR using formerly mentioned empirical relations. Thus we may quantify the effects of randomness and non-linearity resulting from stochastic and systematic properties of sunspot emergence using surface flux transport models.

For each solar cycle, sunspots initially reverse the dipole field of the previous cycle and then establish the opposite polarity of the new cycle. The total dipole moment generated by the emerged sunspots during cycle n is calculated by the sum of the absolute values of the dipole moments at the beginning and the end of cycle n. This allows us to compare the final total dipole moments for cycles with different amplitudes. Despite the large variations in the averaged amplitudes of the three columns in Figure 2, the expected value of the final total dipole moment remains similar. The final total dipole moment is weakly determined by cycle amplitudes due to the effect of nonlinearities. Additionally, the final dipole moments have a large uncertainty range due to the stochastic properties of sunspot emergence, which corresponds to the effects of randomness.

Figure 3 from Jiang (2020) shows the dependence of the final total dipole moment on different cycle strengths. The black solid curve indicates the expected values from 100 surface flux transport simulations using random sunspot group realizations including latitudinal and tilt quenching. They lead to a saturation state in which normal and strong cycles tend to produce similar amounts of the total dipole moment regardless of their amplitudes, whereas weak cycles become even more effective in generating a total dipole moment. The black dashed curve is the curve fit to the black solid curve. The error bars correspond to the 1σ standard deviation, caused by the randomness in the properties of sunspot groups. The shaded region shows the range of the standard deviation. This result paves the way for understanding the nature of solar cycle variability, chaotic or stochastic.

Let's first analyze the effects of nonlinearities without considering the stochastic mechanisms. Based on the fitted relation between the total final dipole moment and the cycle strength along with the calibrated relation between the dipole moment and the subsequent cycle strength (Jiang et al. 2018), with a given cycle n strength S_n, we may determine the strength of the subsequent cycle $n+1$, S_{n+1}. Thus the recursion function of the solar cycle can be derived, which is shown by the black curves of Figure 4. The left panel of the cobweb diagram shows results with different initial conditions in different

https://doi.org/10.1017/S1743921324000097 Published online by Cambridge University Press

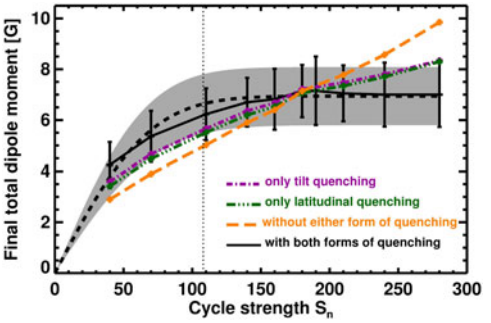

Figure 3. Effects of randomness and non-linearity of sunspot emergence on the solar cycle. The solid black curve shows the expected values from 100 SFT simulations with random sunspot group realisations, including latitude and tilt quenching. The error bars correspond to the 1σ standard deviation caused by the randomness in the sunspot group properties. The shaded area corresponds to the standard deviations. Green dashed triple-dot and purple dashed dot curves show the expected values for SFT simulations with only latitude and tilt quenching, respectively. Orange long dashes show the expected value of SFT simulations without either latitudinal or tilt quenching. Image reproduced with permission from Jiang (2020), copyright by the American Astronomical Society.

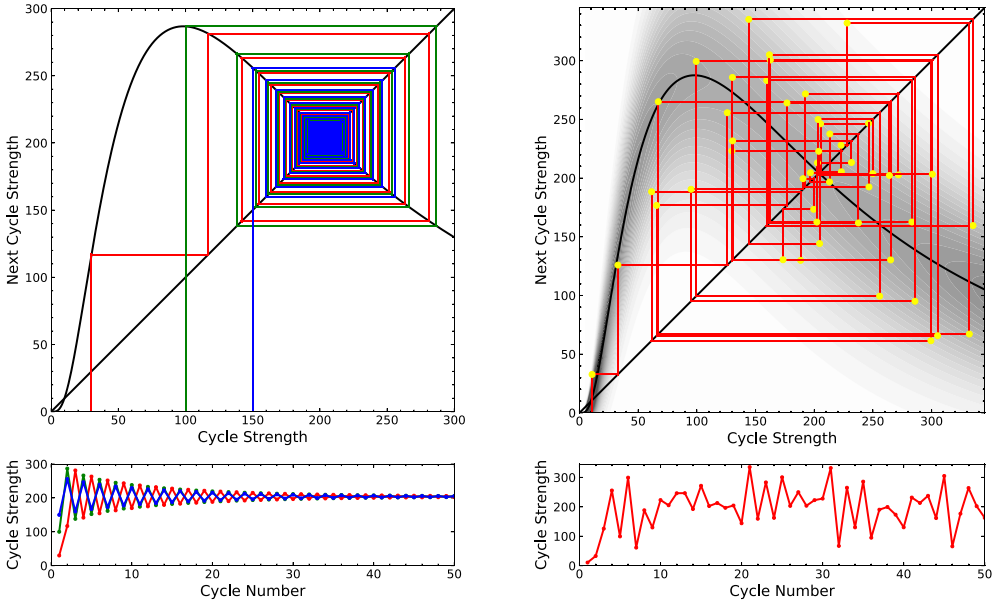

Figure 4. Cobweb diagrams for solar cycle recursion. Left panels: with only nonlinearity. The curves in 3 different colors correspond to different initial conditions. Right panels: with both randomness and nonlinearity. The over-plotted red curve is one random realization.

colors. The lower panel of Figure 4 gives the corresponding solar cycle series. We may see two distinct properties. One is the regular G-O effect at the beginning phase. The other is that the cycle strength eventually reaches a stable fixed point. This implies that the observed nonlinearities lead to a stable limit cycle, rather than a chaotic system (Wang et al. 2024).

Now we include the effect of the randomness in the properties of sunspot groups on the generation of the final total dipole moment. Thus we may generate a large number of

https://doi.org/10.1017/S1743921324000097 Published online by Cambridge University Press

cycles series for analyzing solar cycle variability, especially the G-O effect. The right panel of Figure 4 shows an example of cycle series of 50 cycles. This allows for the analysis of solar cycle variability, including the odd-even effect, through the generation of numerous cycle series. The analysis based on the 1 million synthesized solar cycles indicates that the normalized occurrence frequency of various lengths of G-O blocks follows an exponential distribution, which suggests a Poisson random process. The reconstructed solar cycles of the past 100 cycles by Usoskin et al. (2021), present roughly the same occurrence frequency of the G-O blocks. The nonlinearity contributes to the G-O rule, while the stochastic nature of sunspot emergence causes the probability of obtaining the same even-odd relationship to decrease exponentially as the cycle number increases.

3. Impacts on solar cycle predictions

The aforementioned attempt indicates that the variability of the solar cycle could be attributed to a weakly nonlinear limit cycle affected by stochastic noise. The result is consistent with Cameron and Schüssler (2017), who used a generic normal-form model with parameters constrained by observations. The nature of the solar cycle variability has significant impacts on solar cycle predictions. The dominant effects of randomness put constraints on the scope of the solar cycle prediction. No sensible prediction of the strength of the next cycle can be made before the solar minimum. The uncertain range increases with the scope of the cycle prediction. On the other hand, people need a cycle prediction as early as possible. In this situation, people should keep in mind the uncertain range of dipole moments. Randomness and nonlinearities should be realistically incorporated or considered to get the uncertain range of the dipole moment.

Jiang et al. (2018) developed a scheme to investigate the predictability of the solar cycle over one cycle. There are three main steps. The first is to predict the sunspot emergence of the current cycle using the empirical formulae on the stochastic and systematic properties of sunspot emergence from Jiang et al. (2011). Please note here that the stochastic properties have usually been ignored by prediction models. Ignoring the effect of stochastic properties in sunspot numbers also explains the variable predictions of solar cycle 25 given at different times by Hathaway and Upton †. In January 2022, they once gave the prediction of the maximum amplitude of cycle 25 as less than 100. And the prediction jumped to about 150 in April 2022. From January 2024, their prediction dropped back to about 135. As shown in Figure 3 of Jiang et al. (2018), the prediction of an ongoing cycle using the curve fit to the observed sunspot number has large relative errors, which can be over 50% when it is within 3 years into a cycle. In addition to the uncertainty in the sunspot number, there are also uncertainties in latitude, tilt angle, and area of sunspot emergence, which can significantly affect the sunspot contribution to the polar field.

The second step in investigating the predictability of the solar cycle over one cycle is to utilize the surface flux transport model, with the predicted sunspot group emergence as the flux source, to get the predicted polar field or dipole moment at the cycle minimum. The predicted result includes both the expected value and the uncertain range at cycle minimum. During this step, the observed magnetograms are required as the initial condition. As noted by Cameron et al. (2016); Jiang and Cao (2018), the uncertainty due to measurement error in the magnetogram should also be considered. Upton and Hathaway (2018) once predicted that cycle 25 would be about 95% smaller in strength than cycle 24, and that cycle 25 would be the weakest solar cycle in the last hundred years. Solar behavior has shown that the prediction by Upton and Hathaway (2018) is not the real

† http://solarcyclescience.com/forecasts.html

https://doi.org/10.1017/S1743921324000097 Published online by Cambridge University Press

case. As analyzed by Jiang et al. (2023), the weak prediction is mainly due to the synchronic magnetogram at CR2172 that they used as the initial field. As shown in Figures 4 and 5 of Jiang et al. (2023), the map has some differences from the synoptic magnetogram at CR2172 especially at low latitudes. The flux at low latitudes has a significant effect on the predicted dipole moment at cycle minimum (Wang and Sheeley 1991; Jiang et al. 2014; Petrovay et al. 2020), leading to the weak dipole moment at cycle minimum and hence a weak prediction of cycle 25.

The final step is to obtain a predicted subsequent cycle profile, including its uncertainty, by using a carefully calibrated linear relation between the dipole moment at cycle minimum and the subsequent cycle strength. This step involves using the relation between cycle strength and the averaged cycle profile. It is expected that each real solar cycle will exhibit some deviations from the averaged profile within a certain range.

4. Conclusions

In this paper we argue that a prerequisite for meaningful solar cycle predictions is to understand the nature of solar cycle variability. Unlike atmospheric dynamics for weather forecasting, solar cycle variability could result from a weakly nonlinear limit cycle dominated by stochastic noise. Systematic and stochastic properties of sunspot emergence contribute to the nonlinear and stochastic mechanisms of the solar cycle, respectively. The stochastic properties constrain the scope of the solar cycle prediction. Uncertainty increases with the scope of the prediction. The uncertainties in observed magnetograms and sunspot emergence should be well evaluated and included in the physics-based solar cycle predictions. Otherwise, the models could make misleading predictions as the article mentioned in the last section.

Physics-based solar cycle prediction usually directly or indirectly use the polar field (dipole moment) at cycle minimum as precursor. As shown in Figure 4 of Labonville et al. (2019), some of such predictions gave a weaker cycle 25 than cycle 24. This is mainly due to the fact that the stochastic noise in magnetograms and sunspot formation, or the systematic properties of sunspot formation, have not been well incorporated into the prediction models. Fortunately, Jiang et al. (2018); Pesnell and Schatten (2018); Svalgaard (2020), who also used the precursor, gave different results. The behavior of cycle 25 provides further evidence that the polar field precursor method is reliable.

Acknowledgements. The research is supported by the National Natural Science Foundation of China (Nos. 12173005 and 12350004) and the National Key R&D Program of China No. 2022YFF0503800. The SDO/HMI data are courtesy of NASA and the SDO/HMI team. Wilcox Solar Observatory data used in this study was obtained via the web site `http://wso.stanford.edu` courtesy of J.T. Hoeksema. The sunspot records are courtesy of WDC-SILSO, Royal Observatory of Belgium, Brussels.

References

Babcock, H. W. 1961, The Topology of the Sun's Magnetic Field and the 22-YEAR Cycle. *apj*, 133, 572.

Bhowmik, P., Jiang, J., Upton, L., Lemerle, A., & Nandy, D. 2023, Physical Models for Solar Cycle Predictions. *Space Sci. Rev.*, 219(5), 40.

Cameron, R. H., Jiang, J., & Schüssler, M. 2016, Solar Cycle 25: Another Moderate Cycle? *Astrophys. J. Lett.*, 823(2), L22.

Cameron, R. H. & Schüssler, M. 2017, Understanding Solar Cycle Variability. *Astrophys. J.*, 843(2), 111.

Dasi–Espuig, M., Solanki, S. K., Krivova, N. A., Cameron, R., & Peñuela, T. 2010, Sunspot group tilt angles and the strength of the solar cycle. *Astron. Astrophys.*, 518, A7.

Gnevyshev, M. N. & Ohl, A. I. 1948, On the 22-year cycle of solar activity. *Living Reviews in Solar Physics*, 25, 18.

Howe, R. 2009, Solar Interior Rotation and its Variation. *Living Reviews in Solar Physics*, 6(1), 1.

Jiang, J. 2020, Nonlinear Mechanisms that Regulate the Solar Cycle Amplitude. *Astrophys. J.*, 900(1), 19.

Jiang, J., Cameron, R. H., Schmitt, D., & Schüssler, M. 2011, The solar magnetic field since 1700. I. Characteristics of sunspot group emergence and reconstruction of the butterfly diagram. *Astron. Astrophys.*, 528, A82.

Jiang, J., Cameron, R. H., & Schüssler, M. 2014, Effects of the scatter in sunspot group tilt angles on the large-scale magnetic field at the solar surface. *Astrophysical Journal*, 791(1).

Jiang, J. & Cao, J. 2018, Predicting solar surface large-scale magnetic field of Cycle 24. *Journal of Atmospheric and Solar-Terrestrial Physics*, 176, 34–41.

Jiang, J., Chatterjee, P., & Choudhuri, A. R. 2007, Solar activity forecast with a dynamo model. *Mon. Not. Roy. Astron. Soc.*, 381(4), 1527–1542.

Jiang, J., Hathaway, D. H., Cameron, R. H., Solanki, S. K., Gizon, L., & Upton, L. 2014, Magnetic Flux Transport at the Solar Surface. *Space Sci. Rev.*,.

Jiang, J., Wang, J.-X., Jiao, Q.-R., & Cao, J.-B. 2018, Predictability of the Solar Cycle Over One Cycle. *Astrophys. J.*, 863(2), 159.

Jiang, J., Zhang, Z., & Petrovay, K. 2023, Comparison of physics-based prediction models of solar cycle 25. *Journal of Atmospheric and Solar-Terrestrial Physics*, 243, 106018.

Jiao, Q., Jiang, J., & Wang, Z.-F. 2021, Sunspot tilt angles revisited: Dependence on the solar cycle strength. *Astron. Astrophys.*, 653, A27.

Karak, B. B. 2020, Dynamo Saturation through the Latitudinal Variation of Bipolar Magnetic Regions in the Sun. *Astrophys. J. Lett.*, 901(2), L35.

Labonville, F., Charbonneau, P., & Lemerle, A. 2019, A Dynamo-based Forecast of Solar Cycle 25. *Solar Phys.*, 294(6), 82.

Leighton, R. B. 1969, A Magneto-Kinematic Model of the Solar Cycle. *Astrophys. J.*, 156, 1.

Li, K. J., Wang, J. X., Zhan, L. S., Yun, H. S., Liang, H. F., Zhao, H. J., & Gu, X. M. 2003, On the Latitudinal Distribution of Sunspot Groups over a Solar Cycle. *Solar Phys.*, 215(1), 99–109.

Lorenz, E. N. 1963, Deterministic Nonperiodic Flow. *Journal of Atmospheric Sciences*, 20(2), 130–148.

Lorenz, E. N. 1965, A study of the predictability of a 28-variable atmospheric model. *Tellus*, 17(3), 321–333.

Lorenz, E. N. 1969, The predictability of a flow which possesses many scales of motion. *Tellus*, 21(3), 289–307.

Nandy, D. 2021, Progress in Solar Cycle Predictions: Sunspot Cycles 24-25 in Perspective. *Solar Phys.*, 296(3), 54.

Penza, V., Bertello, L., Cantoresi, M., Criscuoli, S., & Berrilli, F. 2023, Prediction of solar cycle 25: applications and comparison. *Rendiconti Lincei. Scienze Fisiche e Naturali*, 34(3), 663–670.

Pesnell, W. D. & Schatten, K. H. 2018, An Early Prediction of the Amplitude of Solar Cycle 25. *Solar Phys.*, 293(7), 112.

Petrovay, K. 2020, Solar cycle prediction. *Living Reviews in Solar Physics*, 17(1), 2.

Petrovay, K., Nagy, M., & Yeates, A. R. 2020, Towards an algebraic method of solar cycle prediction. I. Calculating the ultimate dipole contributions of individual active regions. *Journal of Space Weather and Space Climate*, 10, 50.

Solanki, S. K., Wenzler, T., & Schmitt, D. 2008, Moments of the latitudinal dependence of the sunspot cycle: a new diagnostic of dynamo models. *Astron. Astrophys.*, 483(2), 623–632.

Svalgaard, L. 2020, Prediction of Solar Cycle 25. *arXiv e-prints*,, arXiv:2010.02370.

Upton, L. A. & Hathaway, D. H. 2018, An Updated Solar Cycle 25 Prediction With AFT: The Modern Minimum. *Geophys. Res. Lett.*, 45(16), 8091–8095.

Usoskin, I. G., Solanki, S. K., Krivova, N. A., Hofer, B., Kovaltsov, G. A., Wacker, L., Brehm, N., & Kromer, B. 2021, Solar cyclic activity over the last millennium reconstructed from annual ^{14}C data. *Astron. Astrophys.*, 649, A141.

Wang, Y. M. & Sheeley, N. R., J. 1991, Magnetic Flux Transport and the Sun's Dipole Moment: New Twists to the Babcock–Leighton Model. *Astrophys. J.*, 375, 761.

Wang, Y. M. & Sheeley, N. R. 2009, Understanding the Geomagnetic Precursor of the Solar Cycle. *Astrophys. J. Lett.*, 694(1), L11–L15.

Wang, Z.-F., Jiang, J., & Wang, J.-X. 2021, Algebraic quantification of an active region contribution to the solar cycle. *Astron. Astrophys.*, 650, A87.

Wang, Z.-F., Jiang, J., & Wang, J.-X. 2024, Algebraic quantification of an active region contribution to the solar cycle. *in prep.*,.

Weber, M. A., Fan, Y., & Miesch, M. S. 2011, The Rise of Active Region Flux Tubes in the Turbulent Solar Convective Envelope. *Astrophys. J.*, 741(1), 11.

Yeates, A. R., Cheung, M. C. M., Jiang, J., Petrovay, K., & Wang, Y.-M. 2023, Surface Flux Transport on the Sun. *Space Sci. Rev.*, 219(4), 31.